

Seasonal Sediment and Diatom Record from Late Holocene Laminated Sediments, Effingham Inlet, British Columbia, Canada

ALICE S. CHANG and R. TIMOTHY PATTERSON

Department of Earth Sciences, Carleton University, Ottawa-Carleton Geoscience Centre,
Ottawa, Ontario, K1S 5B6, Canada, E-mail: asm_chang@yahoo.com

ROGER McNEELY

Geological Survey of Canada, Ottawa, Ontario, K1A 0E8, Canada

PALAIOS, 2003, V. 18, p. 477–494

Laminated diatomaceous sediments from Effingham Inlet, British Columbia, are described and classified in this study. Analyses were made from ten 15-cm long sediment slabs, spanning the last 5500 years, and 52 thin sections from which 408 sedimentary couplets were identified. Microfossil analysis and radiocarbon dating of the sediments reveal that the laminae are annually deposited (i.e., varves), with couplets containing a terrigenous and diatomaceous lamina pair. Terrigenous laminae, averaging 0.56 mm in thickness, consist of silt, organic debris, and robust diatoms, and are deposited during the winter months. Diatomaceous laminae, with a mean thickness of 1.85 mm, can be divided into three component laminae of differing compositions that reflect changing seasonal conditions during the spring, summer, and autumn months. This seasonal succession is seen in 76% of the couplets examined, recurring year after year with variations in couplet thickness and species occurrence. Couplets lacking the succession may represent deposition during periods of low diatom production or years with low seasonality (e.g., El Niño). Variability in couplet styles corroborates climate trends derived from pollen and Neoglacial studies. Sediments older than 4000 yr BP (calibrated radiocarbon dates) contain couplets with a distinct annual succession, and are interpreted to have been deposited during conditions that were warmer than today. Sediments deposited between 2000 to 4000 yr BP also contain couplets with an annual succession, but the laminated intervals are interrupted by brief nonlaminated intervals. The sediments were likely deposited during cooler and wetter conditions than today. Sediments younger than 2000 yr BP were deposited during modern conditions. This study illustrates the effective utility of an ultra high-resolution analysis of laminated sediment records, once proxy indicators are defined, and is important for understanding post-glacial climate evolution along the coast of British Columbia and throughout the northeast Pacific Ocean during the late Holocene.

INTRODUCTION

Laminated hemipelagic sediments represent a high-resolution record of paleoenvironmental change through time. These sediments are formed when there is a season-

ally heterogeneous sediment supply and a lack of physical or biological reworking (Grimm et al., 1996), which are common in coastal upwelling environments along eastern-boundary oceanic currents. Numerous studies have described laminated hemipelagic diatomaceous sediments from several sites, including the Gulf of California (Calvert, 1966; Pike and Kemp, 1996), Santa Barbara Basin (Bull and Kemp, 1995; Grimm et al., 1996, 1997), and Saanich Inlet (Sancetta and Calvert, 1988; Collins, 1997). Relating various depositional processes and seasonal climate variables to the laminated components has been the focus of these studies.

The objective of this paper is to explore the nature of the laminated sediments in Effingham Inlet by examining the laminated fabric and diatom content at an ultra high (i.e., subannual to annual) stratigraphic resolution over specific intervals of core, and to determine whether the laminae were deposited annually. Once the chronology of the sediments is established, and the laminae described and classified, the laminae are put into a seasonal depositional sequence based on sediment texture and known diatom species ecology. The sequence and composition of laminae can be related to changes in local climate and coastal oceanography during the late Holocene along the coast of British Columbia and for the northeast Pacific Ocean in general. A full description of nonlaminated sediments is not treated here.

This project was undertaken as part of a larger study intended to determine the causal factors of pelagic fish stock fluctuations in the northeast Pacific over the last 5000 years. Effingham Inlet was chosen as the study site because it contains anoxic bottom waters in the restricted inner basin of the fjord, finely laminated sediments that are undisturbed by bioturbation, and a record of fish scales. A comparison of the laminated sediments with modern sedimentary flux patterns will allow for an understanding of environmental changes occurring on subannual to longer time scales for both the past and present. This information is important for reconstructing the paleoclimatic and paleoceanographic record for coastal British Columbia and provides an insight into the migratory patterns of fish species in the region.

BACKGROUND

Effingham Inlet

Effingham Inlet is a 15-km long fjord that is located on the southwest coast of Vancouver Island, and opens direct-

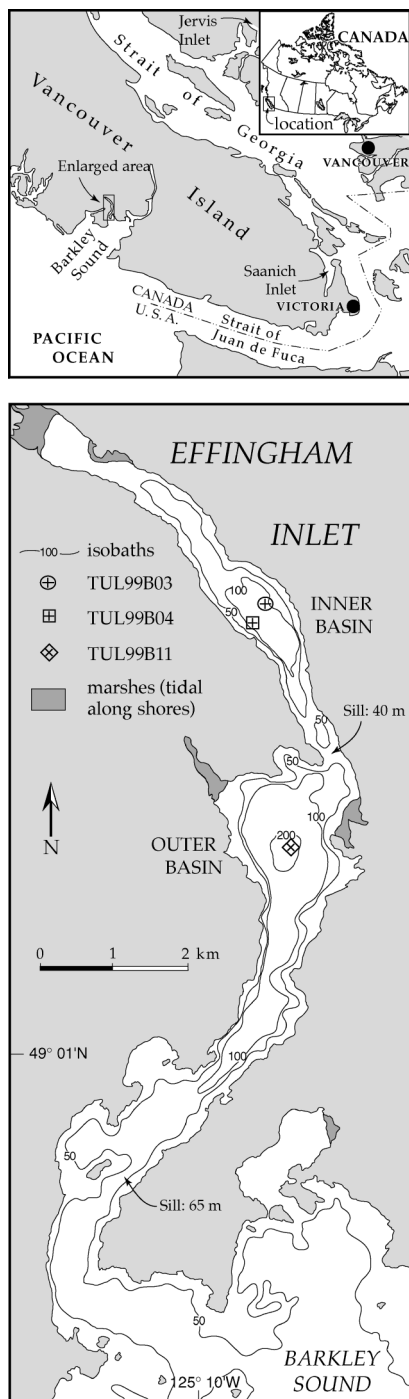


TABLE 1—Descriptive terminology for lamina quality, component abundance estimates, and microfossil preservation criteria.

Quality*	
Distinct	lamina contacts sharp; thickness constant; high color contrast between lamina types
Indistinct	lamina contacts diffuse or gradational; thickness uneven; low color contrast between lamina types
Well-preserved	laminae distinct or indistinct; laterally continuous; no distortion
Poorly preserved	laminae distinct or indistinct; laminae are truncated, distorted or broken
Abundance†	
Abundant	≥50%
Common	>25–50%
Occasional	5–25%
Rare	<5%
Absent	0%
Preservation§	
Excellent	specimens pristine; fine morphological features preserved; no alteration (physical fragmentation or chemical dissolution) of specimens
Good	lightly silicified and robust specimens present; minor alteration
Moderate	lightly silicified specimens present but altered; robust specimens dominate
Poor	lightly silicified specimens absent or rare and altered; robust specimens altered

* Quality of laminae in hand samples and x-radiographs.

† Abundance of components per field of view per lamina in thin section.

§ Preservation of microfossils in thin section.

populations (Barber and Chavez, 1983; Wilkerson et al., 1987; Lange et al., 2000). During strong El Niño events, which occur on average every 10 to 25 years, the effects are propagated poleward through the atmosphere (as teleconnections) or along the coastal ocean (as an oceanic wave guide) where they can impact mid-latitude oceanic regions (Subbotina et al., 2001; R. Thomson, pers. comm., 2002). Other large-scale ocean-atmospheric events, such as the Pacific Decadal Oscillation or shifts in the position and intensity of the Aleutian Low pressure system over the north Pacific, can influence stratification and upwelling, which in turn can affect plankton and pelagic fish abundances (Brodeur and Ware, 1992; Chavez et al., 2003).

METHODS AND MATERIALS

Coring took place in Effingham Inlet in October 1999 on board the CCGS *John P. Tully*. The inner and outer basins were profiled with a 3.5 kHz air gun to locate suitable piston coring sites where the sediment seemed relatively gas-free in the upper few meters. Coring at four sites was carried out in the deepest parts of the basins, and away from the steep sides of the inlet to reduce the incidence of slumped deposits. Four piston cores, each 10 cm in diameter and approximately 11 m in length, were collected from the inner basin, and one core was collected from the outer basin. Additionally, three freeze cores, ranging in length from 1.2 to 2 m, were recovered from the inner basin to locate and characterize the sediment-water interface (Dallimore, 2001). Piston core TUL99B03 (11.4 m in length) was selected for high-resolution analysis because it recovered the highest percentage of visibly distinct laminae of all the cores.

Shell and wood material were extracted from the piston cores and used for accelerated mass spectrometry (AMS) radiocarbon dating. Dating and calibration of the material were performed by the IsoTrace Radiocarbon Laboratory (University of Toronto). The dates were calibrated with the dendrochronologically derived INTCAL98 dataset for

terrestrial material and the MARINE98 dataset for marine material (Stuiver et al., 1998a, b). A shell and wood pair was collected from the outer basin core (TUL99B11) to determine the delta-R marine reservoir correction. Samples from freeze core TUL99B04 (123 cm in length) from a related study were dated using ^{137}Cs and ^{210}Pb at GEOTOP Laboratories (University of Québec at Montréal). Dates for ^{210}Pb activities were calculated using the constant flux-constant sedimentation model (Sorgente et al., 1999).

Locations for sediment slabbing of the piston core were selected based on the quality of the preservation of laminae in order to ensure a high-resolution examination of a variety of representative laminated sequences throughout the core. Ten sediment slabs were extracted from the core perpendicular to laminae using “cookie-cutter” devices that were 15 and 20 cm in length (cf., Schimmelmann et al., 1990; Grimm et al., 1996). The cutters produced slabs measuring 1 cm in thickness and 3 cm in width.

Sediment slabs were x-radiographed to elucidate differences in texture, density, and composition of sedimentary components not readily visible in hand samples. X-radiography was performed on a Faxitron Series 43805-N 110 kV X-ray system at the Geological Survey of Canada (Ottawa). X-rays were shot onto Agfa D7 and D4 strip film, with voltages ranging from 32 to 35 kVp, a constant current of 3.2 mA, and exposure times ranging from 90 to 165 s. The x-radiograph negatives were scanned into a computer and converted into positive images. The positive images were used to corroborate sedimentary descriptions made from hand samples, and to locate laminated sequences for backscattered electron microscopy. Preservation quality of laminae was assessed from the x-radiographs and hand samples (Table 1).

A strip of sediment 0.5 cm in thickness was sliced perpendicular to laminae along the length of each sediment slab and embedded with epoxy resin for the production of a continuous set of thin sections for each slab. Spurr® low-viscosity resin was used for the embedding process (La-

TABLE 2—Radiocarbon dates obtained from core TUL99B03.

Sample number	Lab number	Depth in core (cm)	Material dated	Lithology	Radiocarbon age (yr BP)	Correction 801 \pm 23 yr BP*	Calibrated age (cal yr BP) [†] delta-R = 390 \pm 25 yr (-120 \pm 45 yr)	Calibrated calendar dates [§] delta-R = 390 \pm 25 yr (-120 \pm 45 yr)
RC03S101	TO-8671	97	wood	poorly laminated	160 \pm 40		195 \pm 150	AD 1655–1955
RC03S201	TO-8672	169	shell pair	poorly laminated	1770 \pm 60	969 \pm 83	970 \pm 135 (1495 \pm 160)	AD 895–1165 (AD 345–665)
RC03S301	TO-8673	286	twig	well laminated	2050 \pm 70		1858 \pm 62	BC 80–AD 205
RC03S501	TO-8674	553	twig	laminated	2830 \pm 60		2980 \pm 150	BC 1130–830
RC03S601	TO-8675	822	shell pieces	well laminated	3890 \pm 80	3089 \pm 103	3435 \pm 185 (4085 \pm 245)	BC 1620–1250 (BC 2330–1840)
RC03S701	TO-8676	937	wood	massive	4190 \pm 80		4745 \pm 175	BC 2920–2565

* Correction applied to marine ages after calibrating with delta-R = 390 \pm 25 yr; reported by Robinson and Thomson (1981).

[†] Calibrated age after applying delta-R = 390 \pm 25 yr (Stuiver and Braziunas, 1993) or delta-R = -120 \pm 45 yr (determined from Effingham Inlet outer-basin samples RC11S801A [shell, 2830 \pm 30 yr BP] and RC11S801 [wood, 2570 \pm 60 yr BP])

[§] Calibrated results are reported at the 2-sigma (95% confidence interval) range.

mooureux, 1994). After the epoxy-embedded sediment strips were cured, they were sectioned diagonally into ~3-cm-long pieces with a high-powered bandsaw and highly polished into thin-section slides using conventional techniques. Fifty-two thin sections were produced.

Each thin section was examined by light microscopy (LM). The slides were photographed at a magnification of 12x with a stereomicroscope and a digital camera. Measurements of lamina thickness were made from the magnified images. Thin sections were then examined with a petrographic microscope at magnifications of up to 400x. Diatoms and other microfossils were identified to the lowest taxonomic level when possible. The abundance of microfossils and other particles were assessed semi-quantitatively by visually estimating the percentage proportion of the microfossil or particle per field of view per lamina (Table 1). The percentage estimates and compositions were then used to classify laminae. Preservation status of microfossils was also assessed (Table 1).

Scanning electron microscopy of the sediments was accomplished with a JEOL 6500 scanning electron microscope. Thirty-two thin sections with distinct laminae were examined with backscattered electron microscopy (BSEM), from which high-magnification, cross-sectional images of the laminae were produced. Several tape peels made from the surface of sediment slabs were imaged with scanning electron microscopy (SEM). Topographic images of diatoms and other particles were obtained *in situ* with little disturbance to the sedimentary fabric.

RESULTS

Chronology

Results from AMS radiocarbon dating are reported in Table 2. The established reservoir correction for waters west of Vancouver Island, a delta-R of 320 \pm 25 yr (Stuiver and Braziunas, 1993), was used for the calibration. However, the shell dates yielded ages that were -801 \pm 23 yr too old for marine samples for the region (Dallimore, 2001). The delta-R calculated from the shell and wood pair collected from the outer basin core is -120 \pm 45 yr, which

is different from the accepted value, but the shell and wood were collected 41 cm apart in the core. As a result, calibrated shell dates were not used in the determination of the sediment accumulation rate because the marine reservoir correction has not been definitively established for restricted fjords, such as Effingham Inlet, on the coast of British Columbia (R. Beukens, pers. comm., 2002). The wood date near the top of the core was unreliable because it yielded a wide range of possible ages, and the wood date at the bottom of the core is suspect because it was collected in a massive interval. However, this wood date falls in line with the two wood dates collected in the middle of the core. Using these three wood dates shows that ~5500 years of deposition were recovered in core TUL99B03 (Figure 2A). A linear sediment accumulation rate of 2.25 mm/yr, which was calculated from the regression line drawn through the three calibrated wood dates, shows that the top ~600 yr (~1.4 m) of sediments were not recovered. The number of years not recovered is likely fewer due to the uncompacted nature of the sediment toward the sediment-water interface. An alternate regression line with the same sediment accumulation rate, drawn through all dates calibrated with a delta-R of 390 \pm 25 yr, indicates that only the top ~250 yr (~0.5 m) are missing. This is unlikely since the freeze cores that were recovered are up to 2 m long, and the bottoms of the freeze cores do not overlap stratigraphically with the top of the piston core. The sediment accumulation rate was calculated based on the assumption that gravity-flow deposits added and eroded sediments equally, and that down-core compaction was negligible; hence, the sediment accumulation rate reported here represents an average rate.

Dating of laminated sediments from freeze core TUL99B04 was done by assigning a year to each couplet above a slump deposit known to have been deposited during a 1946, magnitude 7.2 earthquake centered in central Vancouver Island (Rogers, 1980). The year 1963 was determined at a depth of 22.5 cm (Chang et al., 2002). A prominent ¹³⁷Cs peak was also found at this depth and is interpreted as the 1963 peak of atomic testing. The determination of dates from ²¹⁰Pb confirms the position of the

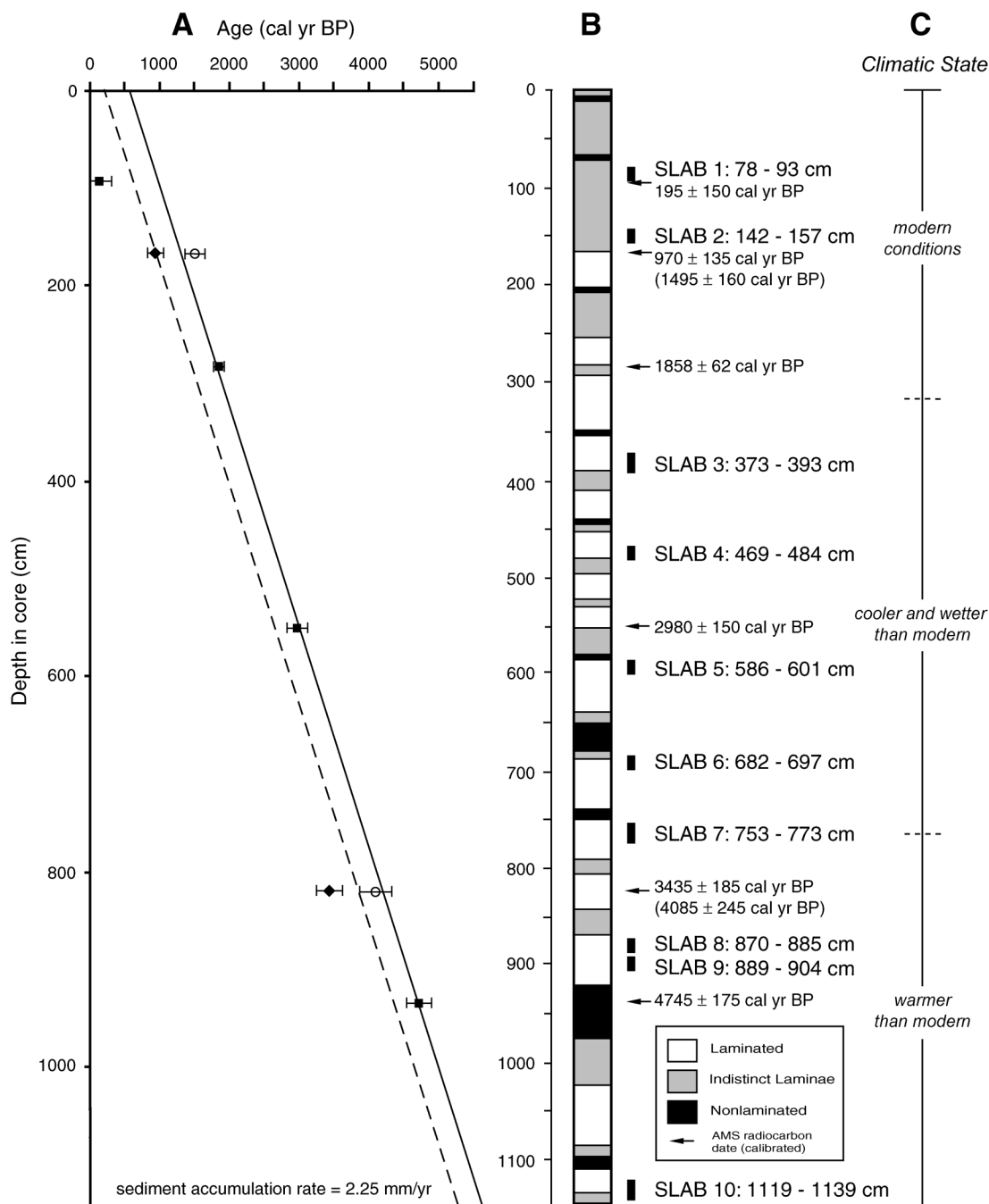


FIGURE 2—Stratigraphic data for piston core TUL99B03. (A) Age-depth relationship for radiocarbon wood dates (black squares) and shell dates (black diamonds) calibrated with $\delta\text{-R}$ of 390 ± 25 yr, and shell dates (open circles) calibrated with $\delta\text{-R}$ of -120 ± 45 yr. Solid regression line runs through three wood dates, and provides sediment accumulation rate and ages used for interpretations throughout this study. Dashed regression line runs through all dates calibrated with $\delta\text{-R}$ of 390 ± 25 yr. (B) Stratigraphic column depicting bulk-sediment fabrics, calibrated radiocarbon dates, and positions of sediment slab samples. Dates in parentheses were calibrated with $\delta\text{-R}$ of -120 ± 45 yr. Nonlaminated intervals represent graded massive beds; indistinctly laminated intervals represent ungraded massive intervals intercalated with poorly laminated intervals. No horizontal scale is implied. (C) Climatic states; see discussion for details.

1963 level and shows that the couplets are annually deposited.

Descriptions from Hand Samples and X-radiographs

The slabs contain well-preserved laminae with couplets containing an olive-green to gray diatomaceous lamina

and a brown terrigenous lamina. Several slabs also contain thin (≤ 2 cm) nonlaminated intervals and intervals of distorted laminae. The sediment was composed mainly of clay- to silt-sized particles (Dallimore, 2001).

In Slab 1, the laminae are indistinct in hand sample and the sediment has a dark-brown color; the laminae are more apparent in the x-ray positive image (Fig. 3). The

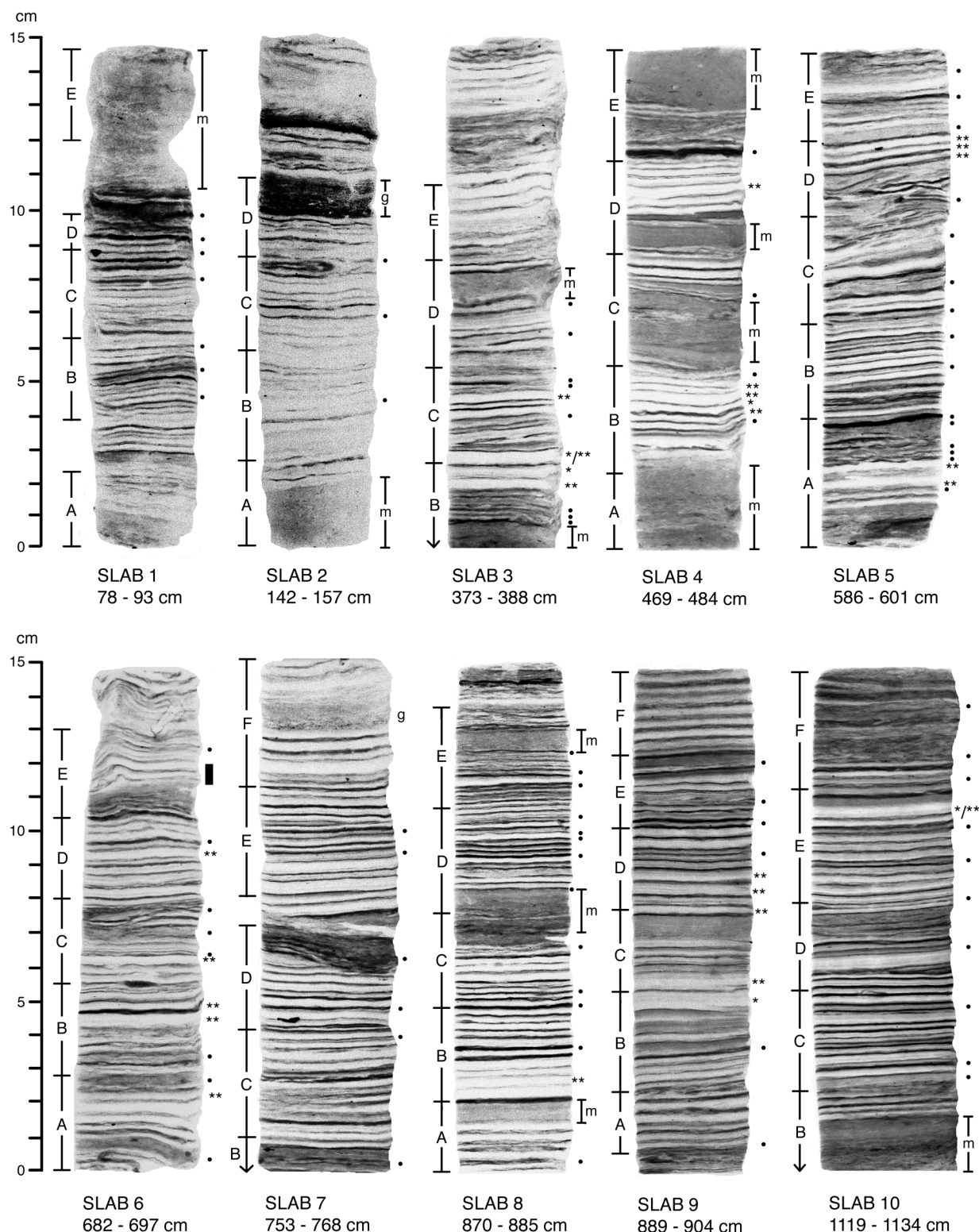


FIGURE 3—X-radiograph positive images of sediment slabs. Only the upper 15 cm of slabs 3, 7, and 10 are pictured; the lower 5 cm of these slabs consisted of a massive interval. See text for descriptions of each slab. Single asterisks denote conspicuously thick *Skeletonema costatum* laminae; double asterisks denote conspicuously thick *Chaetoceros* resting spore laminae. Black dots indicate terrigenous-rich couplets. Intervals labeled "m" represent massive intervals; "g" represents graded beds. Intervals labeled with capital letters represent thin-section intervals; gaps indicate where sediment was damaged during the embedding process. The black bar beside Slab 6 represents the interval where high-magnification imagery was taken (Fig. 10). A magnified image of slide F from Slab 7 is shown in Figure 9.

TABLE 3—Thickness of terrigenous (T) and diatomaceous (D) laminae.

Slab	Lamina type	Number of laminae	Mean lamina thickness (mm) (s.d.)*	Mean couplet thickness (T+D) (mm) (s.d.)
1	T	24	0.73 (0.46)	2.25 (0.69)
	D	24	1.53 (0.67)	
2	T	24	0.52 (0.22)	2.35 (0.88)
	D	25	1.83 (0.78)	
3	T	28	0.70 (0.46)	2.94 (1.30)
	D	28	2.25 (1.42)	
4	T	25	0.55 (0.28)	2.43 (0.86)
	D	26	1.88 (0.70)	
5	T	52	0.60 (0.29)	2.36 (0.87)
	D	52	1.76 (0.88)	
6	T	45	0.69 (0.63)	2.64 (1.04)
	D	45	1.96 (0.97)	
7	T	53	0.56 (0.20)	2.41 (0.87)
	D	53	1.85 (0.80)	
8	T	56	0.42 (0.19)	1.82 (0.71)
	D	56	1.40 (0.70)	
9	T	43	0.48 (0.26)	2.93 (1.23)
	D	43	2.45 (1.02)	
10	T	55	0.52 (0.21)	2.31 (0.88)
	D	56	1.79 (0.84)	
Total	T	405	0.56 (0.35)	2.41 (0.95)
	D	408	1.85 (0.92)	

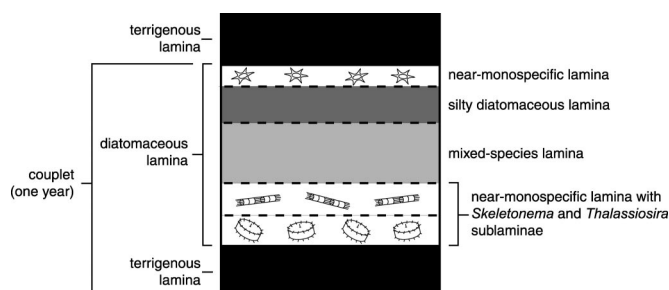
* Standard deviation.

laminae from Slab 2 are more distinct, and contain diatomaceous laminae up to 2 mm thick. The x-rays of slabs 1 and 2 are darker than x-rays of other slabs likely because slabs 1 and 2 came from the wetter and less-consolidated upper sections of the piston core (Fig. 2B).

Laminae from slabs 3 to 10 are more distinct, as is evident from the higher contrast between lamina types in the x-rays (Fig. 3). The sedimentary contacts also are sharper and better defined. Slabs 3 to 7 contain numerous massive intervals and distorted laminae. Slabs 8 to 10 contain well-preserved laminae. Thick, green to olive-green laminae 5 mm thick from slabs 4, 8, 9, and 10 appear as bright bands in the x-rays. Slab 9 has the thickest of the green laminae, with two juxtaposed couplets (Fig. 3). Most slabs show random lamina thickness, but Slab 8 shows a thinning upwards of couplets. Sediment compaction appears to be negligible down the core because the average lamina thickness of each slab is similar, and some of the thicker laminae occur deeper in the core (see Dallimore 2001) (Table 3).

Lamina Description from Thin Sections

Fifty-two thin sections, containing 408 couplets, were examined from a combined total of 142.2 cm of sediment. Diatoms are the most common microfossil in the sediments. Other microfossils, such as fish-scale fragments, coccoliths, radiolaria, planktonic foraminifera, and benthic foraminifera, were observed throughout the sediment in low abundance. Terrigenous laminae have a mean thickness of 0.56 mm ($n = 405$; range: 0.15 mm–3.91 mm). Diatomaceous laminae have a mean thickness of 1.85 mm ($n = 408$; range: 0.20–5.67 mm). The mean thickness of a couplet, calculated from the thickness of all 813 laminae

**FIGURE 4**—Schematic diagram depicting the terminology used to describe laminae in this study. No scale is intended.

measured, is 2.41 mm; mean couplet thickness calculated from each slab varies down the core (Table 3). Terrigenous laminae are fewer in number because they were cut off at the bottom of three thin sections. Diatomaceous laminae can be divided into near-monospecific laminae, mixed-species laminae, and silty diatomaceous laminae (Figure 4). Each lamina type is described in detail below.

Terrigenous Laminae: This type of lamina has a grainy texture and opaque brown color when observed with LM. With BSEM, images appear bright due to numerous dense mineral grains (Fig. 5A, B). Quartz, pyroxene, clay minerals, wood fragments, and organic detritus are abundant. There is also a minor but consistent microfossil component. Diatoms include intact *Paralia sulcata* chains, *Coscinodiscus* spp., *Actinopterychus* spp., *Cyclotella* spp., *Cymbella* spp., *Diploneis* spp., and *Chaetoceros* resting spores. Silicoflagellate species include *Dictyocha speculum* and *Dictyocha fibula*, with *D. speculum* being the more dominant form. Silicoflagellates occur as monospecific blebs and sublaminae. Fragments of diatom valves and girdle bands are common. Preservation of the microfossils ranges from poor to good. The lower contact of terrigenous laminae is gradational whereas the upper contact is sharp.

Near-monospecific Laminae: These laminae consist of clean, excellently preserved diatom frustules. Green particles can be seen inside some diatoms, particularly *Chaetoceros* resting spores (CRS). These particles are likely residual chloroplasts. In BSEM, near-monospecific laminae appear dark due to numerous low-density, resin-filled diatom frustules. Silt and terrigenous-organic detritus are rare to absent. No more than three species (often from the same genus) occur per lamina, with one species dominating $\geq 50\%$ of the assemblage (Fig. 6). Three hundred seventy-two individual near-monospecific laminae and sublaminae were identified from all of the couplets, of which 271 laminae (73%) directly overlie the terrigenous lamina. Dominant taxa in these laminae include *Skeletonema costatum*, CRS, *Thalassiosira nordenskiöldii*, *T. pacifica*, *Thalassionema nitzschioides*, *Odontella longicruris*, and *Ditylum brightwellii*, respectively. Less dominant species include *Asteromphalus* sp., *Coscinodiscus* sp., *Cyclotella* sp., *Odontella aurita*, and *Stephanopyxis turris*, respectively. Laminae also consist of only setae from *Chaetoceros* vegetative cells and diatom girdle bands. Laminae rich in CRS and *S. costatum* can be thick (5 mm), as in Slab 9. Colonial chains of *S. costatum* and *Chaetoceros* spp. are well preserved and can be up to 30 cells in length. Successive

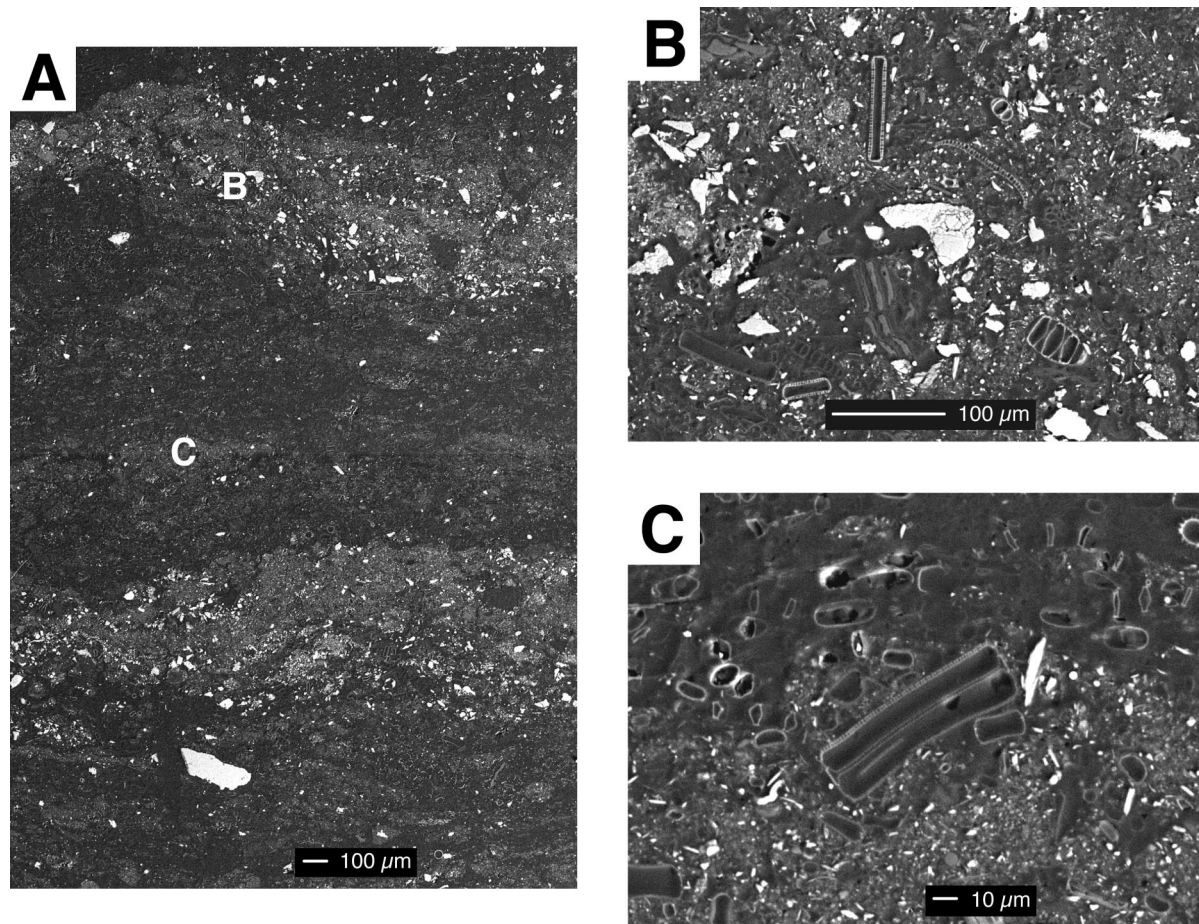


FIGURE 5—BSEM images of terrigenous- and silty-diatomaceous laminae. (A) Photomosaic showing two couplets. The brighter laminae are rich in mineral grains, and the darker laminae are rich in diatoms. Letters B and C indicate where higher magnification images were taken. (B) Close-up view showing detail of terrigenous lamina. Silt grains and robust diatoms are visible. (C) Close-up view showing detail of a silty diatomaceous lamina. This example is rich in finely fragmented diatoms.

sublaminae of different CRS morphologies were observed, with some sublaminae being only a few cells thick. Near-monospecific laminae have a sharp lower contact and a gradational to sharp upper contact.

Mixed-species Laminae: These laminae do not appear as clean as near-monospecific laminae when viewed in LM. In BSEM, the laminae still appear dark unless there is a silt or organic-detritus component (Fig. 7). The proportion of silt and organic detritus ranges from 10–20%. Finely fragmented diatom frustules, or diatom hash (Sancetta, 1989b), are also present. This lamina type can consist of three species (from different genera) with no particular species dominating the assemblage, or more than three species per lamina with one or two taxa slightly dominating the assemblage (i.e., 25–50%). Taxa include *Thalassiosira* spp., *Skeletonema costatum*, *Coscinodiscus* spp., *Actinocyclus* spp., *Asteromphalus* spp., *Thalassionema nitzschioides*, *Thalassiothrix* sp., *Odontella aurita*, *Ditylum brightwellii*, and CRS. Preservation of diatom frustules ranges from moderate to excellent. Both upper and lower contacts of this lamina type are gradational.

Silty Diatomaceous Laminae: These laminae have a composition that is intermediate between mixed-species

laminae and terrigenous laminae. Silt and organic detritus are common (25–50%), but not as abundant as in terrigenous laminae (Fig. 5C). The diatom component is mixed, containing taxa such as *Actinocyclus senarius*, *A. vulgaris*, *Ditylum brightwellii*, *Cyclotella* spp. (Fig. 8A), CRS, and *Thalassionema nitzschioides*. Monospecific blebs and sublaminae of the dinoflagellate cyst *Operculodinium centrocarpum* only occur within silty diatomaceous laminae (Fig. 8B). Silicoflagellate blebs and sublaminae are common (Fig. 8C, D). Near-monospecific sublaminae containing *Skeletonema costatum*, *Thalassionema nitzschioides*, *Ditylum brightwellii*, *Asteromphalus* sp., *Cyclotella* sp., or *Odontella aurita*, can occur within silty diatomaceous laminae. Preservation of the microfossils is poor to good, except in near-monospecific sublaminae where the preservation is moderate to excellent. There is also an occasional component of diatom hash. This hash gives rise to images of unclean diatoms in LM and intermediate brightness in BSEM. Both upper and lower contacts are gradational. This lamina type underlies terrigenous laminae in 67% of all couplets examined. In the remaining couplets, the silty diatomaceous lamina is separated from the over-

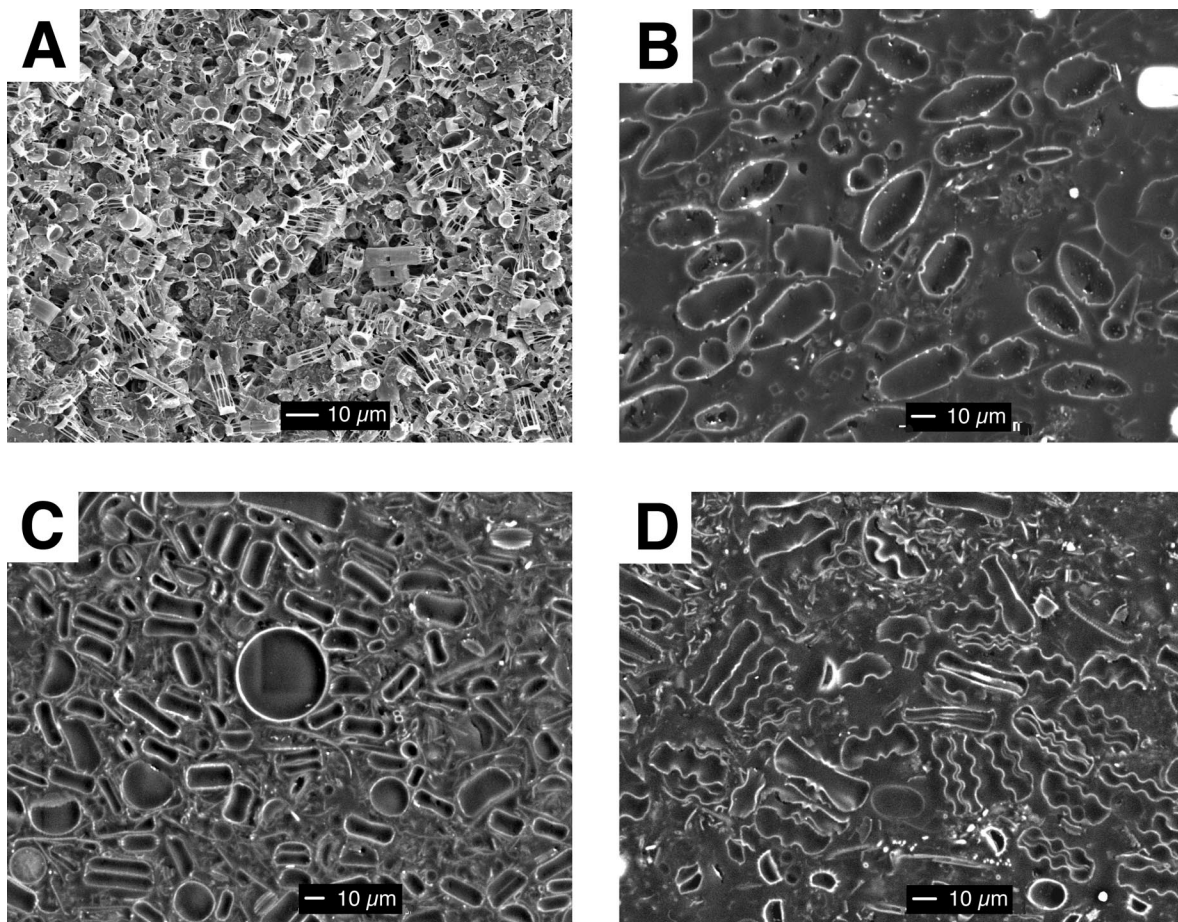


FIGURE 6—Scanning electron images of near-monospecific laminae. 6A was taken by SEM from a tape peel; B–D were taken by BSEM. (A) Pristine *Skeletonema costatum* frustules. (B) *Odontella aurita*. (C) *Thalassiosira* sp. (D) *Asteromphalus* sp.

lying terrigenous laminae by a near-monospecific sublamina or a thin (0.2–0.5 mm) mixed-species lamina.

Depositional Succession of Laminae

Of the 408 couplets examined, 115 couplets (28%) contain the following 4-component succession of laminae, from bottom to top: terrigenous, near-monospecific, mixed-diatom, and silty diatomaceous laminae (Fig. 9). Near-monospecific laminae lying sharply above terrigenous laminae consist of their own distinct internal succession of *Thalassiosira* sp., *Skeletonema costatum*, and *Chaetoceros* spp. sublaminae (Fig. 10). In 56% of 4-component successions, the near-monospecific succession began with a *Thalassiosira* sp. sublamina, followed by *S. costatum* and/or CRS sublaminae. In 30% of 4-component successions, *S. costatum* or CRS sublaminae were lying directly above the terrigenous lamina. In the remaining 14% of couplets, another taxon (e.g., *Odontella* sp., *Ditylum brightwellii*) comprised the near-monospecific laminae overlying the terrigenous lamina.

One hundred ninety-five couplets (~48% of all couplets) contain one of the following 3-component successions, from bottom to top: terrigenous, near-monospecific, and mixed-species or silty diatomaceous laminae; or terrigenous, mixed-species, and silty diatomaceous laminae (Fig.

9). In the first scenario, one or two sublaminae from the *Thalassiosira-Skeletonema-Chaetoceros* sequence are present, but either the mixed-species or silty diatomaceous lamina is absent. In this scenario, 41% of all 3-component couplets had a *Thalassiosira* sp. sublamina lying directly above the terrigenous lamina. Twenty-four percent of all 3-component couplets had either *S. costatum* or a CRS sublamina above the terrigenous lamina. The remaining 3-component successions had another taxon (e.g., *Coscinodiscus* sp., *Odontella longicurvis*, *Ditylum brightwellii*) lying directly above the terrigenous lamina. In the second scenario, the discrete *Thalassiosira-Skeletonema-Chaetoceros* sequence is not present and is replaced by a mixed-species lamina with elevated abundances of *Thalassiosira*, *Skeletonema*, and/or *Chaetoceros* resting spores.

The remaining 98 couplets (24% of all couplets) contain only a 2-component succession of laminae, consisting of a terrigenous lamina and either a mixed diatom or silty diatomaceous lamina.

Downcore Variation

Slabs 6 to 10 from the lower part of the core (~3600 to ~5500 cal yr BP) contain more couplets with the 3- and 4-component lamina succession than slabs from the upper part of the core (~600 to ~3600 cal yr BP) (Fig. 11). The

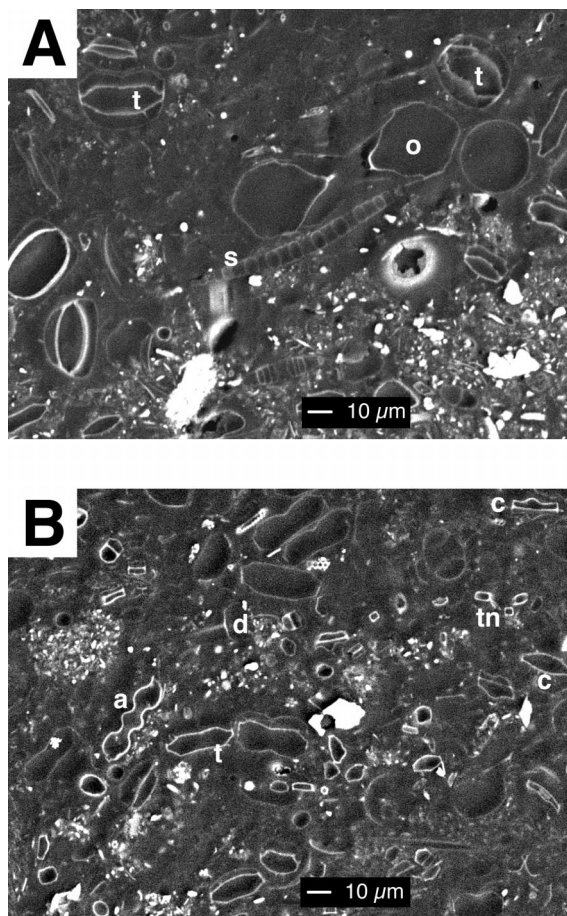


FIGURE 7—Examples of mixed-species laminae. Both images were generated by BSEM. (A) Identifiable diatoms include a chain of *Skeletonema costatum* (s), two connected frustules of *Odontella* sp. (o), and *Thalassiosira nordenskiöldii* (t). Diatom hash and silt grains are also present. (B) Identifiable species include *Thalassiosira nordenskiöldii* (t), square cross-sections of *Thalassionema nitzschioides* (tn), *Asteromphalus* sp. (a), a *Ditylum brightwellii* spine (d), and various morphologies of *Chaetoceros* resting spores (c).

lower part of the core also has more visibly distinct laminae, as is seen from the slab x-radiographs (Fig. 3). Two of the most abundant taxa in the sediments are *Chaetoceros* spp. resting spores and *Skeletonema costatum*. The thickness and occurrence of laminae containing these taxa change within a given slab and throughout the core (Fig. 11E, F). In slabs 9 and 10, CRS laminae are common and *S. costatum* laminae are thicker than in any other slab.

DISCUSSION

Laminated sediments from Effingham Inlet consist of couplets with alternating terrigenous and diatomaceous laminae. The formation of these couplets and their constituent laminae results from the interacting effects of biological production and sediment delivery into the basin. In the following discussion, the annual nature of the laminae is explained, along with the origin of each component lamina.

Determination of the Annual Nature of Laminae

Microfossil evidence shows that the laminated sediments were deposited in a predictable cycle. The repetitive taxonomic succession of diatoms and other microfossils within the 3- and 4-component couplets, and even the sublamina succession of diatom species within a near-mono-specific lamina, reveal that the sediments are deposited annually because similar annual patterns are observed elsewhere in places such as Auke Bay in Alaska (Waite et al., 1992), the Skagerrak in the North Atlantic (Lange et al., 1992), and Saanich and Jervis inlets in British Columbia (Sancetta, 1989a; McQuoid and Hobson, 1997). A three-stage annual succession for planktonic diatoms was first described by Margelef (1958) and modified by Guillard and Kilham (1977). Stage I is characterized by fast-growing diatom species where *Thalassiosira* spp. initiate the bloom, followed by *Skeletonema costatum* and *Chaetoceros* spp. once water temperatures increase. Stage II is characterized by a mixed assemblage of larger diatom species and resting spores. Stage III is characterized by a mixed assemblage of slow-growing large species indicative of late-summer to autumn production.

Determination of couplet thickness as measured from the thin-section images, and calculation of a mean sediment-accumulation rate from calibrated radiocarbon dates, support the annual depositional time scale. If a sedimentary couplet represents one year of deposition, then a comparison between the mean couplet thickness of 2.41 mm (Table 3) and the mean sediment accumulation rate of 2.25 mm/yr (Figure 2A) implies that the couplets in Effingham Inlet are annually deposited. The average couplet thickness from each slab varies about the mean rate derived from radiocarbon dating (Table 3). Dating of recent laminated sediments from freeze core TUL99B04 near the sediment-water interface, using ^{137}Cs , ^{210}Pb , and couplet counting, also shows that the laminae are annual (Chang et al., 2002). Now that the couplets have been established as being annually deposited, the seasonal and ecological character of individual laminae and sublaminas can be described.

Origin of Terrigenous Laminae

Terrigenous laminae in Effingham Inlet are deposited mainly during the late autumn and winter months when increased rainfall leads to increased runoff. Sources of terrigenous material delivery into the inner basin include the Effingham River and a small, unnamed stream leading into the inner basin (Dallimore, 2001). Numerous ephemeral, precipitation-dependent waterfalls on the steep sides of the inlet probably transport a significant, yet ungauged, amount of freshwater input and detritus into the basin. The occurrence of thin (≤ 0.2 mm) terrigenous laminae within a diatomaceous lamina suite may record significant spring or summer precipitation events.

The assemblage of microfossils within terrigenous laminae contains species derived from environments outside the inlet or washed off from the margins of the inlet. The chain-forming diatom *Paralia sulcata* is often observed in terrigenous laminae. McQuoid and Hobson (1998) found *P. sulcata* in plankton records from Saanich Inlet during winter months. They suggested that *P. sulcata* could easily

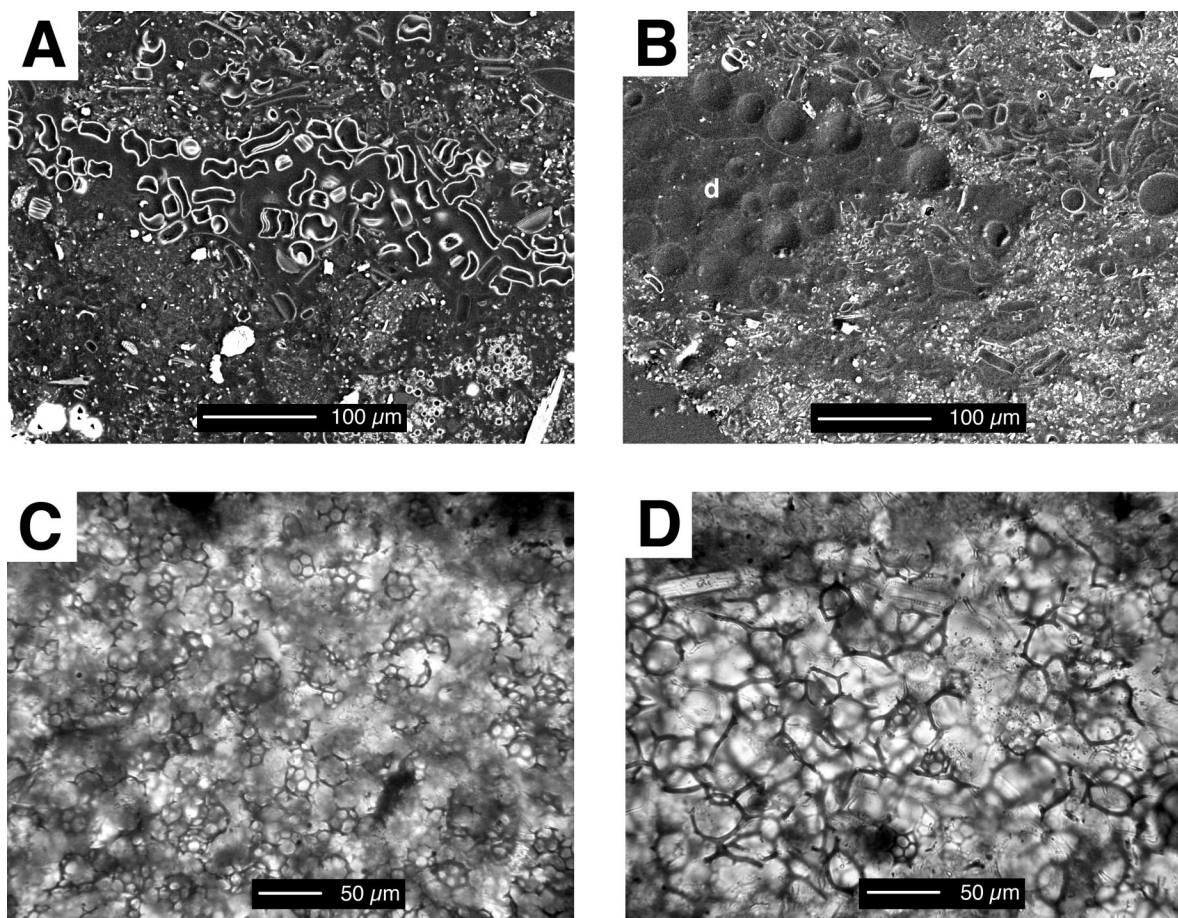


FIGURE 8—Examples of near-monospecific sublaminar and blebs from silty diatomaceous laminae. A and B were taken by BSEM; C and D were taken by LM. (A) Sublamina of *Cyclotella* sp. within silty diatom hash. (B) Bleb of *Operculodinium centrocarpum* dinoflagellate cysts (d) within diatom hash. (C) Monospecific bleb of the silicoflagellate *Dictyocha speculum*. Similar blebs are found in terrigenous laminae. (D) Near-monospecific bleb of the silicoflagellate *Dictyocha fibula* with a few *D. speculum* skeletons.

be sloughed off from the benthos by increased storm activity during the winter, leading to the dispersal of seed populations. Cells then can be stirred into the plankton by winter runoff and storm waves (McQuoid and Hobson, 1998). Genera such as *Cymbella* and *Diploneis* include freshwater species that can enter the inlet during winter runoff from rivers. The presence of coastal neritic and benthic taxa, such as *Actinopterychus*, suggests that sediments have been reworked from the shelf and carried into the inlet (Pike and Kemp, 1996; McQuoid and Hobson, 1997). Silicoflagellates are common in terrigenous laminae. Sautter and Sancetta (1992) found that the maximum abundance of silicoflagellates in sediment traps from San Pedro Basin off the southern Californian Bight occurred during the winter, and attributed their presence to the intrusion of pelagic waters into the basin. Similar conditions may occur in Effingham Inlet.

Origin of Near-monospecific Laminae

The occurrence of near-monospecific laminae that lie directly above terrigenous laminae can be attributed to the annual spring bloom. The spring bloom can be divided into several events—each a response to changing environmental conditions as the bloom progresses. The sharp contact

between near-monospecific laminae and terrigenous laminae likely reflects the onset of the spring bloom in response to a probable combination of events, including increased sunlight, temperature, and the infusion of nutrients into the surface waters via coastal upwelling (Margalef, 1958; Guillard and Kilham, 1977).

In 35% of all couplets examined, *Thalassiosira* species were the first taxa to appear in the Effingham Inlet spring bloom, followed by the appearance of *Skeletonema costatum* and/or different species of CRS. In Auke Bay, *Thalassiosira* species such as *T. aestivalis*, *T. nordenskioldii*, and *T. gravida*, which can tolerate low water temperatures (1 to 5 °C), tend to initiate the bloom as soon as light levels increase in the early spring (Guillard and Kilham, 1977; Waite et al., 1992). *Skeletonema costatum* and *Chaetoceros* spp. then appear later in the spring as the water temperature rises and nitrate is consumed by *Thalassiosira* (Waite et al. 1992). In 20% of couplets examined, *S. costatum* or CRS were the first taxa to appear above the terrigenous lamina, perhaps indicating a warmer spring with temperatures above 5 °C. The appearance of *Thalassiosira* spp., *S. costatum*, and *Chaetoceros* spp. sublaminar in Effingham Inlet sediments is consistent with Stage I of the seasonal succession outlined by Margalef (1958) and Guillard and Kilham (1977) (Fig. 12A).

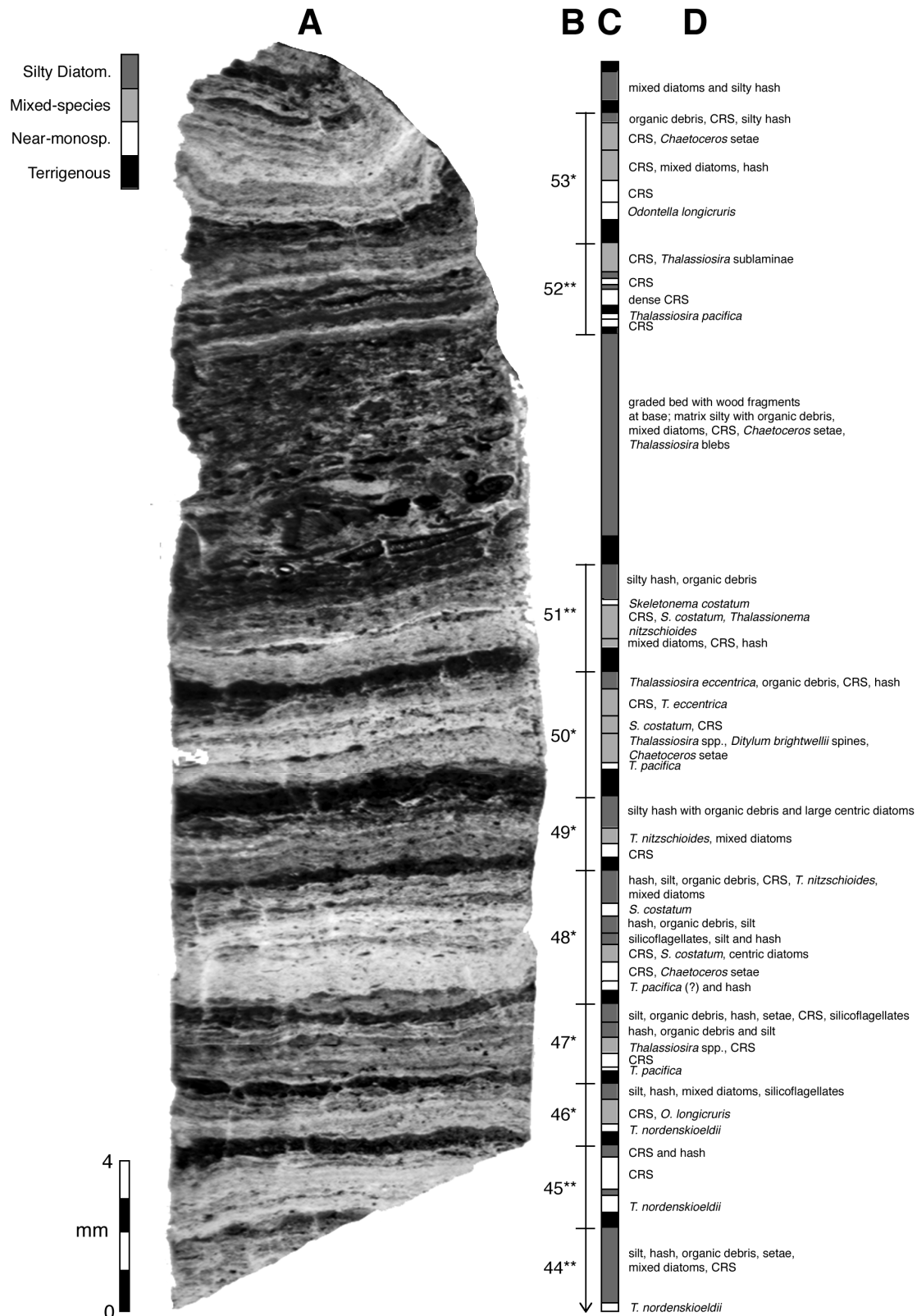


FIGURE 9—Thin-section image from the top of Slab 7 (Fig. 3), showing examples of seasonal succession, and a 6-mm thick, graded massive interval. (A) Photomicrograph of the thin section. (B) Couplet number and succession type. Single asterisk denotes a 4-component succession; double asterisk denotes a 3-component succession. (C) Lamina type. (D) Description of major components within each lamina, with the most abundant component listed first.

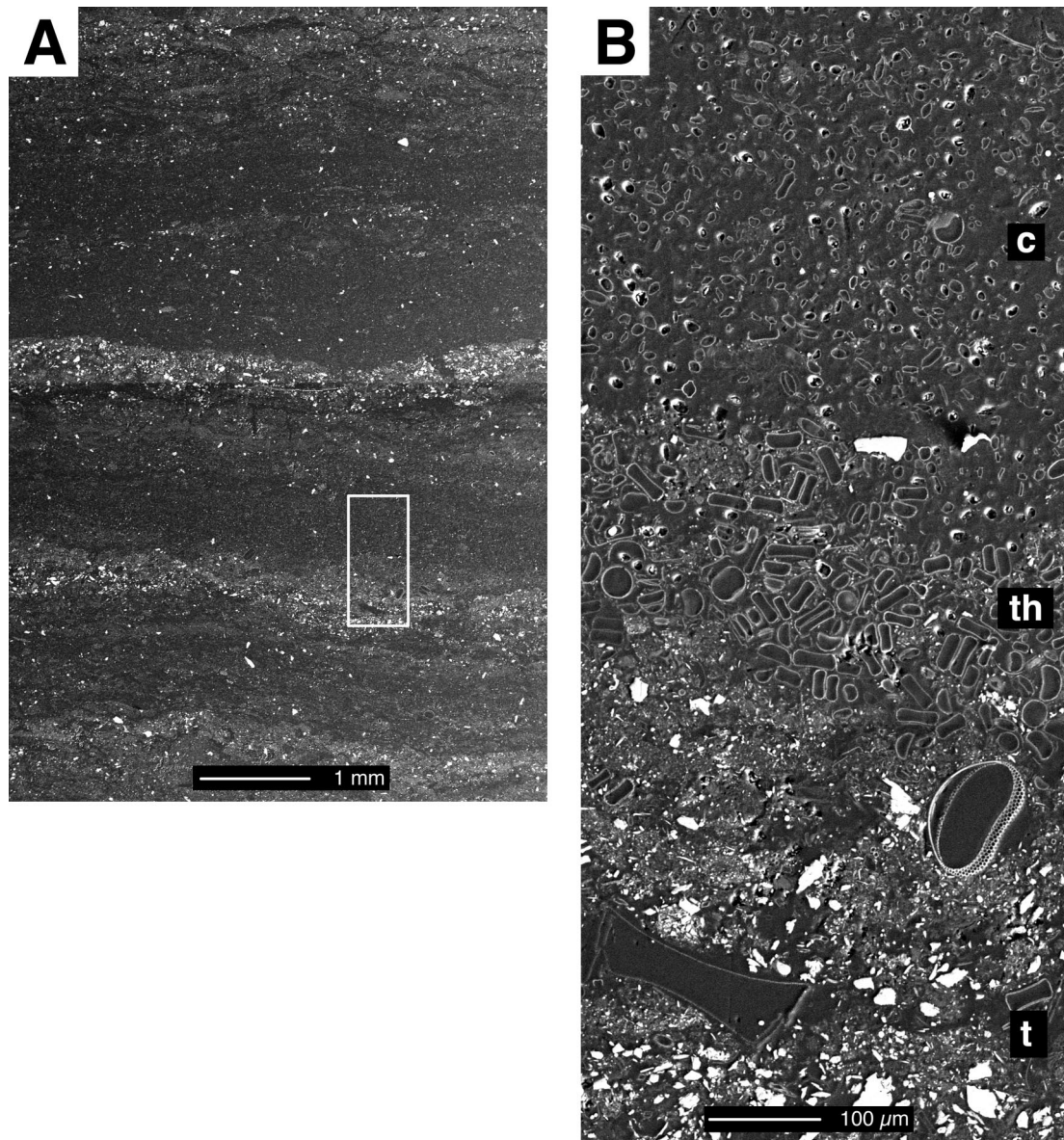


FIGURE 10—BSEM photomosaics of magnified area from Slab 6 (Fig. 3). (A) Low-magnification image showing three couplets. (B) High-magnification image showing seasonal succession of a terrigenous lamina (t), a *Thalassiosira* sp. sublamina (th), and a sublamina enriched with *Chaetoceros* resting spores (c) with a minor component of *Thalassiosira nordenskiöldii*.

The excellent preservation of frustules in near-monospecific laminae is attributed to three possible conditions: (1) diatom proliferation exceeded zooplankton grazing pressure, or grazing was absent (Smayda, 1973); (2) diatoms were exported rapidly from the photic zone via biologically mediated flocculation and self-sedimentation (Grimm et al., 1996, 1997), and bypassed grazing or dissolution in the water column (Silver and Alldredge, 1981; Alldredge and Gotschalk, 1989); and (3) dissolution after burial was minimal, as is the case in Saanich inlet (see Nissembaum et al., 1972). Further *in situ* observations will be required to test which condition, or combination of conditions, is at work in Effingham Inlet for near-monospecific laminae to be preserved.

Near-monospecific sublaminae occurring above or within silty diatomaceous laminae may represent deposition from a late-summer or autumn production event. Sancetta (1989a) found a distinct autumn (September to October) assemblage in Saanich Inlet, consisting of *Thalassionema nitzschioides*, *Rhizosolenia* spp., *Skeletonema costatum*, and *Chaetoceros* spp. Larger diatoms, along with silicoflagellates and dinoflagellates, occurring at this time of year likely are able to grow slowly under nutrient-poor, low-light conditions, or can regulate their buoyancy to acquire nutrients at depth (Guillard and Kilham, 1977; Kemp et al., 2000). These late-summer and autumn laminae may represent deposition of “fall dump” assemblages (Kemp et al., 2000). Alternatively, periodic disturbances to the

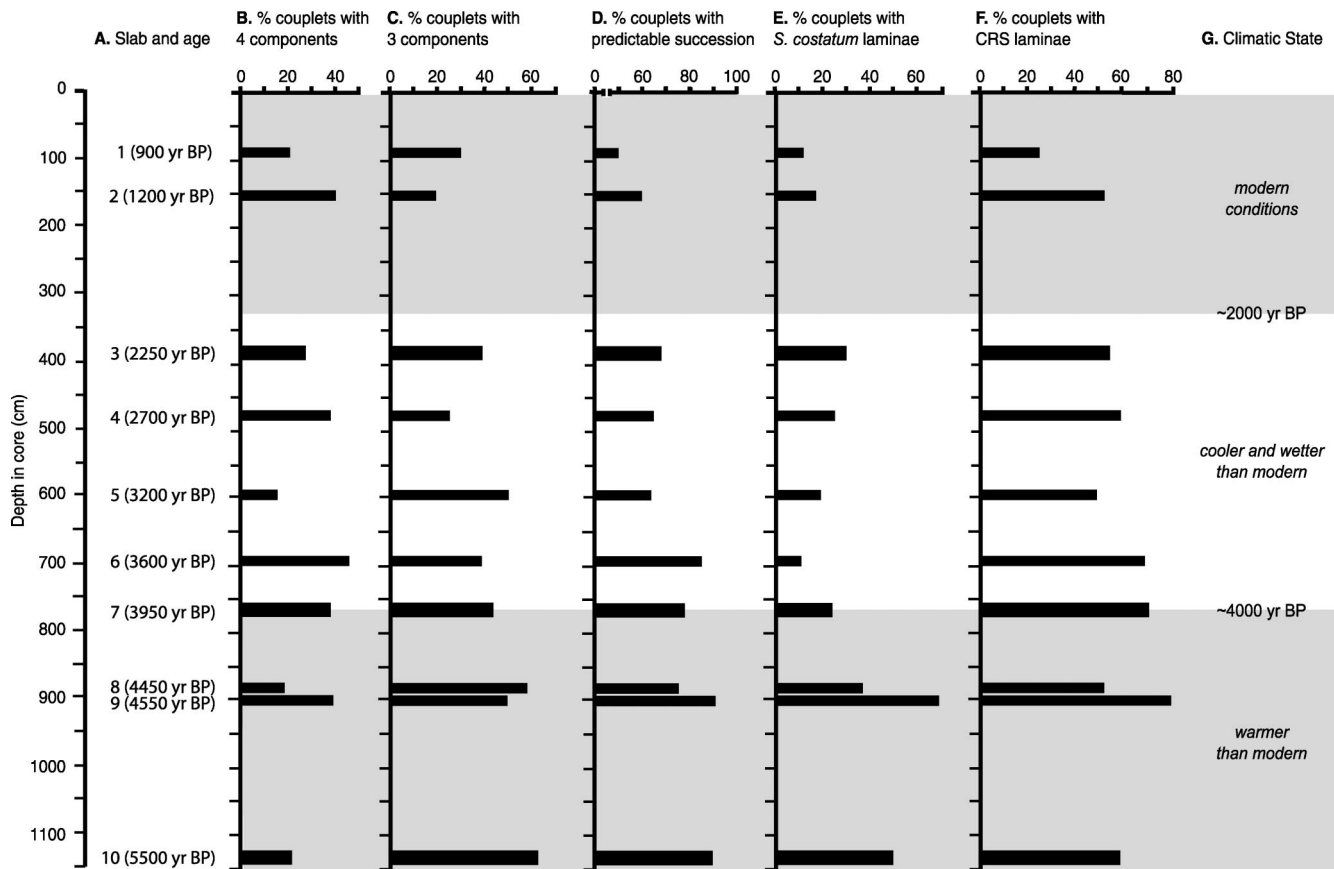


FIGURE 11—Downcore trends of couplet styles and lamina compositions. Climatic states from Hebda (1995).

stratified waters (by storms or strong winds) can bring nutrients back to the surface and lead to diatom miniblooms (Harrison et al., 1983; Haigh et al., 1992).

Origin of Mixed-species Laminae

Mixed-species laminae contain a diverse assemblage of larger diatoms and CRS, and are consistent with Stage II of the seasonal succession described by Margalef (1958) and Guillard and Kilham (1977) (Fig. 12). The species types and preservation status are characteristic of production and deposition during the late-spring to summer months. Diatom hash may represent fragmentation by zooplankton grazing as zooplankton populations catch up with the diatom bloom, or as a function of summer flora being more lightly silicified and susceptible to fragmentation (Sancetta, 1989a). The gradational lower contact of this lamina type in Effingham Inlet may represent deposition reflecting the waning spring bloom and the gradual phasing in of a mixed, high-diversity assemblage from the late spring to autumn seasons.

Origin of Silty Diatomaceous Laminae

The occurrence of oligotrophic, fall-dump species confirms that silty diatomaceous laminae were deposited after the main spring and summer blooms had waned. The presence of silicoflagellates and dinoflagellate cysts in these laminae further suggests that production and depo-

sition occurred mainly in the autumn. Silicoflagellates have been described from Saanich Inlet and Santa Barbara Basin trap studies during the autumn (Sancetta, 1989a; Lange et al., 1997), and dinoflagellates, although rare, were found in autumn sediment trap samples from Jervis Inlet (Sancetta, 1989a).

The mixed assemblage of large diatoms, along with the appearance of silicoflagellates and dinoflagellates, is consistent with the description of Stage III of the seasonal succession (Margalef, 1958; Guillard and Kilham, 1977) (Fig. 12). The gradational upper and lower contacts of silty diatomaceous laminae may represent the gradual increase of silt and organic debris, reflecting an increase in precipitation and terrigenous runoff into the basin during the autumn.

Variability in the Seasonal Succession

The thickness of a terrigenous lamina with respect to a diatomaceous lamina in a given couplet is a function of the amount of terrigenous influx (which depends on the timing and intensity of rainfall) and the intensity of diatom production (which depends on the amount of sunlight, water temperature, and nutrient levels). Couplets exhibiting the recognizable 3- or 4-component seasonal succession are inferred to represent normal years of deposition or years with strong seasonality (Chang et al., 1998). Under these conditions, the majority of rainfall occurs during the

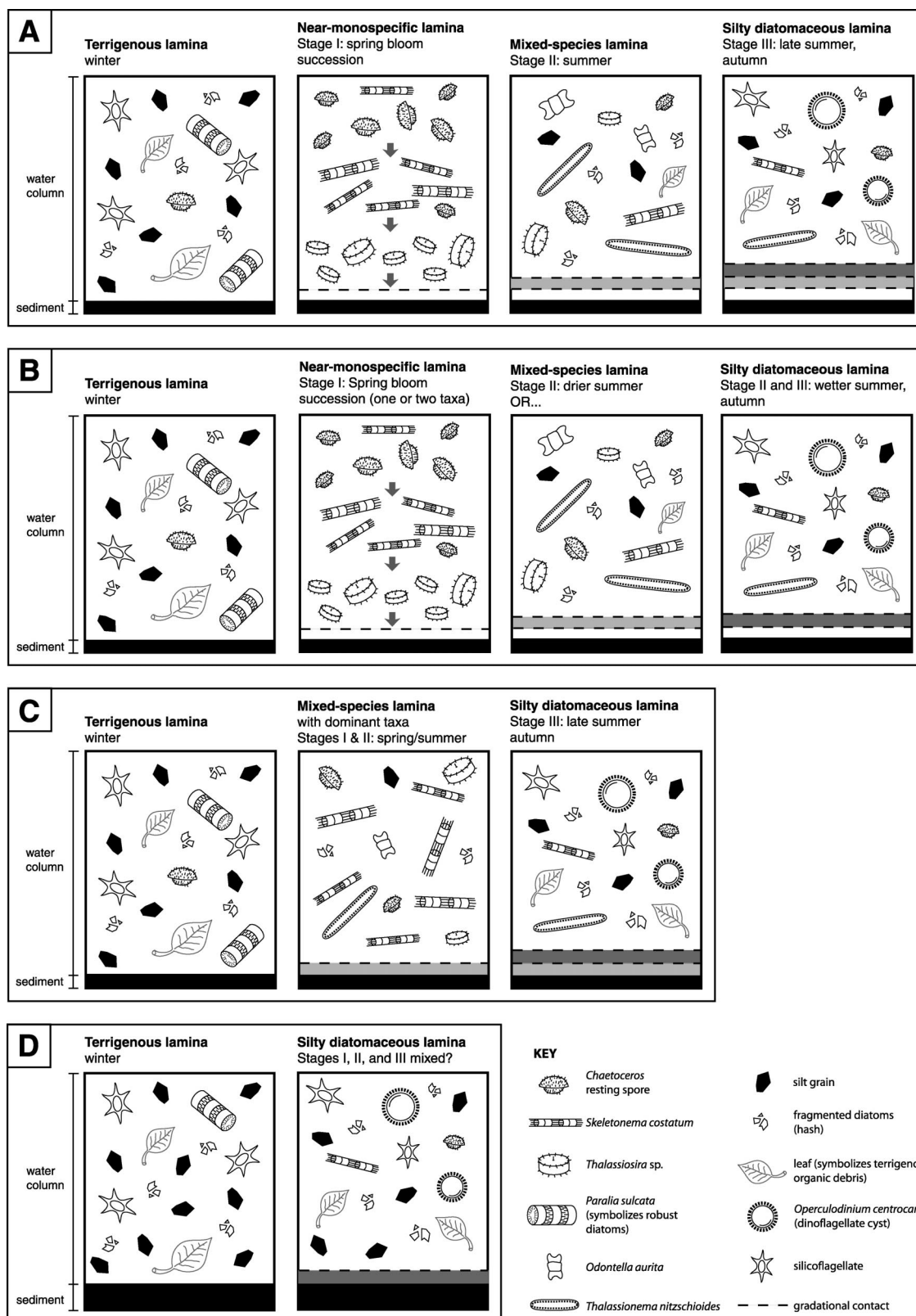


FIGURE 12—Model showing the formation of different annual couplet successions. No scale is intended, however the proportion of each particle type symbolizes their relative abundance as seen in the thin sections (Table 1). (A) Four-component succession. This example shows Stage I with separate *Thalassiosira*, *Skeletonema*, and *Chaetoceros* blooming events. (B) Three-component succession, Scenario 1. (C) Three-component succession, Scenario 2. Stages I and II are mixed together, although there is an elevated occurrence of a spring-bloom taxon, represented here by *Skeletonema*. (D) Two-component succession exemplified by a thick terrigenous lamina and a silty diatomaceous lamina with increased silt and organic content.

autumn and winter, and the spring and summer are relatively dry during which diatom blooms occur.

Twenty-eight percent of the couplets examined contain the well-defined 4-component succession, with at least one, two, or all three of the *Thalassiosira*, *Skeletonema* or CRS sublaminae present directly above the terrigenous lamina (Fig. 12A). Preservation of the *Thalassiosira-Skeletonema-Chaetoceros* sequence may represent discrete blooms of each of these taxa, and stability of the water column near the sediment-water interface in order for the sublaminae to become preserved (i.e., no bottom-water currents or mixing).

Conversely, 48% of the couplets examined contain the 3-component succession. In scenario 1, a succession with only a silty diatomaceous lamina directly above the near-monospecific lamina may signify a wetter summer, and an absent silty diatomaceous lamina may signify a drier autumn (Fig. 12B). In scenario 2 (Fig. 12C), the presence of a mixed-species lamina and a lack of a near-monospecific lamina may represent mixing of taxa in the water column, or be the result of monospecific sublaminae that were reworked or mixed at the sediment-water interface by bottom-water currents. Apart from these differences, the 3-component succession is otherwise similar to the 4-component succession in its record of seasonal flux of particles.

Couplets lacking the recognizable succession (i.e., 2-component couplets or 3-component couplets possessing anomalously thick (2–3 mm) terrigenous and silty diatomaceous laminae and a thin (0.2 mm) near-monospecific lamina) may record abnormal years, or years of weak seasonality (Fig. 12D). An analysis of the couplets from thin sections reveals that terrigenous-rich 2- and 3-component couplets occur on average every 3–20 years, although there can be a bundle of up to 3 successive couplets with abundant terrigenous debris (Fig. 3). El Niño conditions may be responsible for the lowered diatom abundance and increased terrigenous debris in some of these couplets. Diatomaceous laminae also may be masked by elevated deposition of terrigenous material (see Sancetta, 1996) as a consequence of higher rainfall, which often accompanies major El Niño phenomenon in this region. Analysis of freeze core TUL99B04 indicates that during El Niño years (e.g., 1951–1952, 1976–1977, and 1982–1983), terrigenous laminae are thicker and absolute diatom concentrations are lower. The cyclicity of El Niño and other ocean-atmosphere phenomenon is the topic of continuing research, which will include statistical and time-series analyses of a ~12,000-year sediment record obtained in Effingham Inlet during the International Marine Past Global Changes (IMAGES) coring program in May 2002 (R. Thomson and T. Pedersen, pers. comm., 2002).

Paleoenvironmental Interpretation

Downcore trends in the observed characteristics of slab lithologies and microfossil content (represented by laminae with abundant *Skeletonema costatum* and CRS) were compared to local and regional climate change in Vancouver Island as interpreted from pollen and Neoglacial records. The timing of climatic intervals listed below indicates approximate ages, as the transition from one climate state to another lasted for as much as 1500 to 2000 years (Mathewes and Heusser, 1981).

Slabs 6 to 10 (~3600 to 5500 cal yr BP) contain the most couplets with the seasonal succession and laminae containing CRS and *S. costatum* (Fig. 11). This evidence infers that constant climatic conditions favorable to annual seasonal upwelling, and light levels sufficient enough to sustain healthy annual diatom blooms were present prior to ~3600 cal yr BP. In particular, slabs 8 to 10 (4400 to 5500 cal yr BP) contain the most distinctly laminated intervals in the entire core. Seasonality was apparently strong during this time and conditions favored the proliferation of fast-growing, spring-bloom species. The inlet likely experienced consistently anoxic conditions during this interval, resulting in the distinctly laminated character of slabs 8 to 10. The pollen record suggests that prior to ~4000 yr BP, climate conditions were warmer and drier than they are today (Hebda, 1995; Fig. 2C and 11G), with the Holocene Hypsithermal event occurring at ~6000 ka.

In contrast, slabs 1 to 5 (~900 to ~3100 cal yr BP) have fewer couplets with the seasonal succession and a relatively lower number of couplets containing CRS and *S. costatum*. This may indicate a slight decrease in primary production and hence decreased delivery of nutrients to the coastal ocean from recent times to ~3100 cal yr BP.

Nonlaminated intervals are common in slabs 3 to 7 (~2200 to ~4000 cal yr BP), indicating a departure during this time from the normally anoxic conditions that are conducive to the preservation of laminated sediments. Results from continuing research show that on rare occasions it is possible for the bottom waters of the inner basin to be aerated briefly by deeply upwelled and oxygenated waters (Dallimore, 2001). These waters enter along the bottom of the inlet either in the winter during Arctic outbreak conditions, or early in the annual spring upwelling season during a rare combination of weak tidal currents in the inlet, significant rainfall, and strong (>10 m/s) northeasterly winds (Thomson, 1981; Griffin and Leblond, 1989). Therefore, the higher incidence of nonlaminated units in slabs 3 to 7 may indicate that precipitation was likely higher at this time. Indeed, wetter conditions are indicated by the pollen record from 2000 to 4000 yr BP for this region of Vancouver Island (Hebda, 1995). Additionally, this interval coincides with the mid-Neoglacial advance of the Tiedemann glacier (3300 to 1900 cal yr BP) in the Coast Mountains, with the advance a likely response to climate deterioration after the Holocene Hypsithermal (Ryder and Thomson, 1986). This interval also contains some of the thickest diatomaceous laminae found throughout the core (Table 3, Fig. 3). These thick diatomaceous laminae occur in discrete packets of 7- to 10-year intervals and may represent isolated cycles of increased biological production and climate instability.

The frequency at which couplets with a high terrigenous content occurs does not appear to fluctuate greatly throughout the three time periods (Fig. 3). If these couplets represent deposition during possible El Niño years, then further research is required in order to determine the frequency and intensity of El Niño cycles during the late Holocene along the coast of British Columbia.

CONCLUSIONS

This study indicates that variations in the annual sequence of lamina components are proxies for changes in

primary production and precipitation, factors which themselves are proxies for climate and nutrient supply to the coastal ocean, which in turn can be related to coastal-ocean dynamics. The results show that the late Holocene climate varied substantially in this region. Primary production was highest and persistent anoxia of the bottom waters occurred prior to ~4000 yr BP, with cooler and wetter conditions than present occurring between ~2000 and 4000 yr BP, after which modern conditions were established.

A distinctive seasonal succession of diatom species observed in the sediments agrees well with observations made by Margalef (1958) and Guillard and Kilham (1977) for marine planktonic diatoms. This evidence, along with isotopic dating of the sediments, shows that the laminated sediments in Effingham Inlet are annually deposited. El Niño cycles also may be recorded in the sediment where highly terrigenous couplets occur every 3–20 years in the slabs examined. The determination of annual and longer cycles from the sediments is important for the ongoing work of detecting trends in the abundance of pelagic fish species along the British Columbia coast.

The next step in continuing research in Effingham Inlet is being taken toward a full understanding of the annual diatom depositional cycle and diatom ecology, by comparing late Holocene sediments with modern sediment-trap data, weather records, and El Niño records for Effingham Inlet and the surrounding region. The determination of quantitative diatom abundances from each season will pinpoint the timing and strength of the production of various species and identify the modern environmental triggers for each event. This is important for modeling and reconstructing a continuous high-resolution climate record for southwestern British Columbia and the northeast Pacific Ocean in general for the late Holocene. With global climate change and its effects a growing concern, a thorough understanding of past environmental trends is vital for projecting future climate fluctuations.

ACKNOWLEDGEMENTS

We would like to thank R.E. Thomson, A. Prokoph, A. Dallimore, A. Wolfe, J. Pike, and two anonymous reviewers for providing constructive comments to improve this paper. We thank A. Kumar for identifying dinoflagellate cysts; M. Bertram for preliminary discussions of her sediment trap work; R. Beukens, for discussions about radiocarbon dating; and S. Spaulding, R. Hall, and R. Telford for discussions about chloroplasts. We are grateful to Captain Frost and the crew of the CCGS *John P. Tully*. This study was funded by grants from the Natural Sciences and Engineering Research Council of Canada (NSERC) and the Canadian Foundation for Climatic and Atmospheric Sciences (CFCAS) to RTP; as well as grants to ASC from the Cushman Foundation for Foraminiferal Research, the Geological Society of America, and the Ontario Graduate Scholarship Program (Ontario Ministry of Training, Colleges and Universities, Canada).

REFERENCES

ALLDREDGE, A.L., and GOTSCHALK, C.C., 1989, Direct observations of the mass flocculation of diatom blooms: characteristics, settling

- velocities and formation of diatom aggregates: Deep-Sea Research, v. 36, p. 159–171.
- BARBER, R.T., and CHAVEZ, F.P., 1983, Biological consequences of El Niño: Science, v. 222, p. 1203–1210.
- BORNHOLD, B.D., FIRTH, J.V., ADAMSON, L.M., BALDAUF, J.G., BLAIS, A.P., ELVERT, M., FOX, P.J., HEBDA, R., KEMP, A.E.S., MORAN, K., MORFORD, J.H., MOSHER, D.C., PRARIE, Y.T., RUSSELL, A.D., SCHULTHEISS, P., and WHITICAR, M.J., 1998, Leg 169S, Sites 1033 and 1034, Saanich Inlet: Proceedings of the Ocean Drilling Program, Initial Reports, v. 169S: Ocean Drilling Program, College Station, Texas, 138 p.
- BRODEUR, R.D., and WARE, D.M., 1992, Long-term variability in zooplankton biomass in the subarctic Pacific Ocean: Fisheries Oceanography, v. 1, p. 32–38.
- BULL, D., and KEMP, A.E.S., 1995, Composition and origins of laminae in Late Quaternary and Holocene sediments from the Santa Barbara Basin: in Kennett, J.P., Baldauf, J.G., and Lyle, M., eds., Proceedings of the Ocean Drilling Program, Scientific Results, v. 146: Ocean Drilling Program, College Station, Texas, p. 77–87.
- CALVERT, S.E., 1966, Origin of diatom-rich, varved sediments from the Gulf of California: Journal of Geology, v. 74, p. 546–565.
- CHANG, A.S., GRIMM, K.A., and WHITE, L.D., 1998, Diatomaceous sediments from the Miocene Monterey Formation, California: a lamina-scale investigation of biological, ecological and sedimentary processes: PALAIOS, v. 13, p. 439–458.
- CHANG, A.S., HAY, M.B., PROKOPH, A., and PATTERSON, R.T., 2002, High-resolution diatom productivity and cyclostratigraphy (1946–1993) from Effingham Inlet, British Columbia, Canada: 17th International Diatom Symposium, Book of Abstracts, p. 21.
- CHAVEZ, F.P., RYAN, J., LLUCH-COTA, S.E., and NIQUEN, C.M., 2003, From anchovies to sardines and back: multidecadal change in the Pacific Ocean: Science, v. 299, p. 217–221.
- COLLINS, A.D., 1997, Interannual variability of laminated sediment and its relationship to climate, Saanich Inlet, B.C.: Unpublished M.S. Thesis, University of Victoria, Victoria, 233 p.
- DALLIMORE, A., 2001, Late Holocene geologic, oceanographic and climate history of an anoxic fjord; Effingham Inlet, west coast Vancouver Island: Unpublished Ph.D. Dissertation, Carleton University, Ottawa, 465 p.
- GRIFFIN, D.A., and LEBLOND, P.H., 1990, Estuary/ocean exchange controlled by spring-neap tidal mixing: Estuarine and Coastal Shelf Science, v. 30, p. 275–297.
- GRIMM, K.A., LANGE, C.B., and GILL, A.S., 1996, Biological forcing of hemipelagic sedimentary laminae: evidence from ODP Site 893, Santa Barbara Basin, California: Journal of Sedimentary Research, v. 66, p. 613–624.
- GRIMM, K.A., LANGE, C.B., and GILL, A.S., 1997, Self-sedimentation of fossil phytoplankton blooms in the geologic record: Sedimentary Geology, v. 110, p. 151–161.
- GUILLARD, R.R.L., and KILHAM, P., 1977, The ecology of marine planktic diatoms: in Werner, D., ed., The Biology of Diatoms: Botanical Monographs, v. 13: Blackwell Scientific Publications, New York, p. 372–469.
- HAIGH, R., TAYLOR, F.J.R., and SUTHERLAND, T.F., 1992, Phytoplankton ecology of Sechart Inlet, a fjord system on the British Columbia coast. I. General features of the nano- and microplankton: Marine Ecology Progress Series, v. 89, p. 117–134.
- HARRISON, P.J., FULTON, J.D., TAYLOR, F.J.R., and PARSONS, T.R., 1983, Review of the biological oceanography of the Strait of Georgia: pelagic environment: Canadian Journal of Fisheries and Aquatic Sciences, v. 40, p. 1064–1094.
- HEBDA, R.J., 1995, British Columbia vegetation and climate history with focus on 6 ka BP: Géographie Physique et Quaternaire, v. 49, p. 55–79.
- KEMP, A.E.S., PIKE, J., PEARCE, R.B., and LANGE, C.B., 2000, The “fall dump”—a new perspective on the role of a “shade flora” in the annual cycle of diatom production and export flux: Deep-Sea Research II, v. 47, p. 2129–2154.
- LAMOUREUX, S.F., 1994, Embedding unfrozen lake sediments for thin section preparation: Journal of Paleolimnology, v. 10, p. 141–146.
- LANGE, C.B., HASLE, G.R., and SYVERTSEN, E.E., 1992, Seasonal cycle of diatoms in the Skagerrak, North Atlantic, with emphasis on the period 1980–1990: Sarsia, v. 77, p. 173–187.

- LANGE, C.B., WEINHEIMER, A.L., REID, F.M.H., TAPPA, E., and THUNELL, R.C., 2000, Response of siliceous microplankton from the Santa Barbara Basin to the 1997–1998 El Niño event: California Cooperative Oceanic Fisheries Investigations (CalCOFI) Report, v. 41, p. 186–193.
- LANGE, C.B., WEINHEIMER, A.L., REID, F.M.H., and THUNELL, R.C., 1997, Sedimentation patterns of diatoms, radiolarians, and silicoflagellates in Santa Barbara Basin, California: California Cooperative Oceanic Fisheries Investigations (CalCOFI) Report, v. 38, p. 161–170.
- MARGALEF, R., 1958, Temporal succession and spatial heterogeneity in phytoplankton: in Traverso, A.A., ed., Perspectives in Marine Biology: University of California Press, Berkeley, p. 323–249.
- MATHEWES, R.W., and HEUSSER, L., 1981, A 12,000 year palynological record of temperature and precipitation trends in southwestern British Columbia: Canadian Journal of Botany, v. 59, p. 707–710.
- MCQUOID, M.R., and HOBSON, L.A., 1997, A 91-year record of seasonal and interannual variability of diatoms from laminated sediments in Saanich Inlet, British Columbia: Journal of Plankton Research, v. 19, p. 173–194.
- MCQUOID, M.R., and HOBSON, L.A., 1998, Assessment of palaeoenvironmental conditions on southern Vancouver Island, British Columbia, Canada, using the marine tycho plankton *Paralia sulcata*: Diatom Research, v. 13, p. 311–321.
- MCQUOID, M.R., and HOBSON, L.A., 2001, A Holocene record of diatom and silicoflagellate microfossils in sediments of Saanich Inlet, ODP Leg 169S: Marine Geology, v. 174, p. 111–124.
- NISSEBAUM, A., PRESLEY, B.J., and KAPLAN, I.R., 1972, Early diagenesis in a reducing fjord, Saanich Inlet, British Columbia. I. Chemical and isotopic changes in major components of interstitial water: Geochimica et Cosmochimica Acta, v. 36, p. 1007–1027.
- PATTERSON, R.T., GUILBAULT, J.-P., and THOMSON, R.E., 2000, Oxygen level control on foraminiferal distribution in Effingham Inlet, Vancouver Island, British Columbia, Canada: Journal of Foraminiferal Research, v. 30, p. 321–335.
- PIKE, J., and KEMP, A.E.S., 1996, Records of seasonal flux in Holocene laminated sediments, Gulf of California: in Kemp, A.E.S., ed., Palaeoclimatology and Palaeoceanography from Laminated Sediments: Geological Society (London) Special Publication No. v. 116, p. 157–169.
- ROBINSON, S.N., and THOMSON, R.E., 1981, Radiocarbon corrections for marine shell dates with application to southern Pacific northwest coast prehistory: Syesis, v. 14, p. 45–57.
- ROGERS, G.C., 1980, A documentation of soil failure during the British Columbia earthquake of 23 June 1946: Canadian Geotechnical Journal, v. 17, p. 122–127.
- RYDER, J.M., 1989, Climate (Canadian Cordillera): in Fulton, R.J., ed., Quaternary Geology of Canada and Greenland, Geology of Canada, No. 1: Geological Survey of Canada, Ottawa, p. 26–31.
- RYDER, J.M., and THOMSON, R.E., 1986, Neoglaciation in the southern Coast Mountains of British Columbia: chronology prior to the late Neoglacial maximum: Canadian Journal of Earth Sciences, v. 23, p. 273–287.
- SANCETTA, C., 1989a, Spatial and temporal trends of diatom flux in British Columbian fjords: Journal of Plankton Research, v. 11, p. 503–520.
- SANCETTA, C., 1989b, Processes controlling the accumulation of diatoms in sediments: a model derived from British Columbia fjords: Paleooceanography, v. 4, p. 235–251.
- SANCETTA, C., 1996, Laminated diatomaceous sediments: controls on formation and strategies for analyses: in Kemp, A.E.S., ed., Palaeoclimatology and Palaeoceanography from Laminated Sediments: Geological Society (London) Special Publication, No. 116, p. 17–21.
- SANCETTA, C., and CALVERT, S.E., 1988, The annual cycle of sedimentation in Saanich Inlet, British Columbia: implications for the interpretation of diatom fossil assemblages: Deep-Sea Research, v. 35, p. 71–90.
- SAUTTER, L.R., and SANCETTA, C., 1992, Seasonal associations of phytoplankton and planktic foraminifera in an upwelling region and their contribution to the seafloor: Marine Micropaleontology, v. 18, p. 263–278.
- SCHIMMELMANN, A., LANGE, C.B., and BERGER, W.H., 1990, Climatically controlled marker layers in Santa Barbara Basin Sediments, and fine-scale core-to-core correlation: Limnology and Oceanography, v. 35, p. 165–173.
- SILVER, M., and ALLDREDGE, A., 1981, Bathypelagic marine snow: deep-sea algal and detrital community: Journal of Marine Research, v. 39, p. 501–530.
- SMAYDA, T.J., 1973, The growth of *Skeletonema costatum* during a winter-spring bloom in Narragansett Bay: Norwegian Journal of Botany, v. 20, p. 219–247.
- SORGENTE, D., FRIGNANI, M., LONGONE, L., and RAVAIOLI, M., 1999, Chronology of Marine Sediments: Interpretation of Activity-Depth Profiles of ^{210}Pb and other Radioactive Tracers, Part I: Technical Report n. 54: Consiglio Nazionale delle Ricerche Istituto per la Geologia Marina Bologna, 32 p.
- STRONACH, J.A., NG, M.K., FOREMAN, M.G., and MURTY, T.S., 1993, Tides and currents in Barkley Sound and Alberni Inlet: Marine Geodesy, v. 16, p. 1–41.
- STUIVER, M., and BRAZIUNAS, T.F., 1993, Radiocarbon and ^{14}C ages of marine samples to 10,000 B.C.: Radiocarbon, v. 35, p. 137–189.
- STUIVER, M., REIMER, P.J., BARD, E., BECK, J.W., BURR, G.S., HUGHEN, K.A., KROMER, B., MCCORMAC, F.G., PLICHT, J., and SPURK, M., 1998a, INTCAL98 radiocarbon age calibration 24,000–0 cal BP: Radiocarbon, v. 40, p. 1041–1083.
- STUIVER, M., REIMER, P.J., and BRAZIUNAS, T.F., 1998b, High-precision radiocarbon age calibration for terrestrial and marine samples: Radiocarbon, v. 40, p. 1127–1151.
- SUBBOTINA, M.M., THOMSON, R.E., and RABINOVICH, A.B., 2001, Spectral characteristics of sea level variability along the west coast of North America during the 1982–83 and 1997–98 El Niño events: Progress in Oceanography, v. 49, p. 353–372.
- THOMSON, R.E., 1981, Oceanography of the British Columbia Coast: Canadian Special Publication of Fisheries and Aquatic Sciences No. 56, Ottawa, 291 p.
- THOMSON, R.E., and GOWER, J.F.R., 1998, A basin-scale instability event in the Gulf of Alaska: Journal of Geophysical Research, v. 103, p. 3033–3040.
- THOMSON, R.E., HICKEY, B.M., and LEBLOND, P.H., 1989, The Vancouver Island Coastal Current: fisheries barrier and conduit: in Beamish, R.J., and MacFarlane, G.A., eds., Effects of Ocean Variability on Recruitment and an Evaluation of Parameters Used in Stock Assessment Models: Canadian Special Publication of Fisheries and Aquatic Sciences No. 108, Ottawa, p. 265–296.
- WAITE, A., BIENFANG, P.K., and HARRISON, P.J., 1992, Spring bloom sedimentation in a subarctic ecosystem. II. Succession and sedimentation: Marine Biology, v. 114, p. 131–138.
- WILKERSON, F.P., DUGDALE, R.C., and BARBER, R.T., 1987, Effects of El Niño on new, regenerated, and total production in eastern boundary upwelling systems: Journal of Geophysical Research, v. 92(C13), p. 14,347–14,353.

ACCEPTED JUNE 23, 2003

